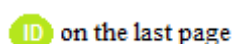




Adsorption of basic red 2 dye by activated biomass charcoal in batch and column systems

Bilal ACEMİOĞLU^{1,*}, Neslihan KARATAŞ¹, Melike Hilal GÜLER¹, Murat ERTAŞ²,

Mehmet Hakkı ALMA³



¹Department of Chemistry, Faculty of Science and Arts, Kilis 7 Aralık University, 79000, Turkey

²Department of Forest Industry Engineering, Faculty of Forestry, Bursa Technical University, 16310, Turkey

³Department of Forest Industry Engineering, Faculty of Forest, Kahramanmaraş Sutcu Imam University, 46060/Rectorate of Iğdır University, Iğdır, 76000, Turkey

Received: 24 November 2019; Revised: 09 December 2019; Accepted: 10 December 2019

*Corresponding author e-mail: acemioğlu@kilis.edu.tr

Citation: Acemioğlu, B.; Karataş, N.; Güler, M. H.; Ertaş, M.; Alma, M. H. *Int. J. Chem. Technol.* 2019, 3 (2), 136-145.

ABSTRACT

Activated biomass charcoal produced from peanut shells was utilized as an adsorbent for the removal of basic red 2 (BR2) dye from aqueous solution in batch and column systems. In batch system, the effects of shaking time, initial BR2 concentration, solution pH and temperature on the adsorption were studied. While the adsorption was increasing with increasing contact time, initial BR2 concentration and temperature, it decreased with increasing solution pH. In column system, the effects of solution flow rate and initial BR2 concentration were investigated. The adsorption of BR2 was determined between 82.40 and 99.91% under all conditions such as concentration, temperature and pH for batch system. The column adsorption was found as 99.50%. Adsorption obeyed the Freundlich isotherm and the pseudo-second order kinetic model. SEM and FT-IR studies indicated that a surface adsorption might probably be occurred on the heterogeneous surface of activated biomass charcoal.

Keywords: Peanut shell charcoal, basic red 2, adsorption, column.

Bazık kırmızı 2 boyasının kesikli ve kolon sistemlerinde aktifleştirilmiş biyokütle kömürü tarafından adsorpsiyonu

ÖZ

Yerfıstığı kabuklarından üretilen aktifleştirilmiş biyokütle kömürü, kesikli ve kolon sisteminde bazık kırmızı 2 (BR2) boyasının sulu çözeltiden uzaklaştırılması için bir adsorbent olarak kullanıldı. Kesikli sistemde adsorpsiyon üzerine çalkalama süresi, başlangıç BR2 konsantrasyonu, çözelti pH'sı ve sıcaklığın etkileri incelendi. Adsorpsiyon temas süresi, başlangıç BR2 konsantrasyonu ve sıcaklık ile artarken artan çözelti pH'sı ile azaldı. Kolon sisteminde çözelti akış hızı ve başlangıç BR2 konsantrasyonunun etkileri incelendi. Kesikli sistem için, konsantrasyon, sıcaklık ve pH gibi tüm şartlar altında BR2 adsorpsiyonu %82.40 ve %99.91 arasında belirlendi. Kolon adsorpsiyonu ise %99.50 olarak bulundu. Adsorpsiyon Freundlich izotermi ve sözde ikinci dereceden kinetik modele uyum gösterdi. SEM ve FT-IR incelemeleri, aktifleştirilmiş biyokütle kömürün heterojen yüzeyinde bir yüzey adsorpsiyonunun meydana gelmiş olabileceğine işaret etti.

Anahtar Kelimeler: Yerfıstığı kabuğu kömürü, bazık kırmızı 2, adsorpsiyon, kolon.

1. INTRODUCTION

Matrix structural molecules comprising lignin, cellulose and hemicellulose are known as lignocellulosic materials. Such substances generally constitute the class of forest origin and agricultural wastes. For example, tree

barks,¹⁻⁴ tree leaves/leaves,⁵⁻⁷ wood sawdust,⁸⁻¹² fruit peels/shell,¹³⁻¹⁶ pirina or olive oil wastes/olive pomace/olive stone,¹⁷⁻²¹ shells of hard-shelled fruits such as walnut, almond, hazelnut,²²⁻²⁴ husks and straws of cereals such as wheat, barley,²⁵ peanut shell,²⁶⁻²⁹

vineyard pruning wastes,³⁰ are agricultural lignocellulosic waste materials. As alternative to activated carbon, these materials have commonly been used as adsorbents in removing the metals and dyes from aqueous medium. Of these low cost waste materials, with use of peanut shell, some works have been reported for metal and dye adsorption in the literature. For instance, peanut shell pretreated with HCl has been utilized as an adsorbent for remazol brilliant blue R removal.³¹

For instance, basic red 2 (BR2) adsorption by peanut shell has been worked by Sakalar and co-workers.²⁷ In another study, peanut shell has been utilized as an adsorbent for remazol orange RGB removal from aqueous solution.²⁸ On the other hand, some alternative materials produced from peanut shell have also been used as adsorbents for dye adsorption. For example, polyurethane-type foam fabricated from peanut shell has been utilized for the sorption of remazol brilliant blue R³² and safranin-O dyes³³ Moreover, sodium hydroxide-activated biochar produced from peanut shell has been used as an adsorbent for remazol orange RGB removal.³⁴ Herein, activated biomass charcoal produced from peanut shell has been utilized as an adsorbent to remove BR2, a cationic dye, from aqueous medium by adsorption. Such a study has not been done before, and therefore this work is original. The effects of shaking time (ie. the contact time of adsorbent with dye solution), initial dye concentration, pH and temperature on the adsorption process have been studied. Moreover, column adsorption study, SEM and FT-IR analyses has also been performed. All results obtained have been interpreted in detail.

2. MATERIALS AND METHODS

2.1. Materials

2.1.1. Adsorbent charcoal

Peanut shell wastes as raw material for the production of adsorbent charcoal were taken from Osmaniye province of Turkey. Firstly it was washed and dried in an oven. Then, the dried peanut shells were powdered by a crusher and sieved throughout a 100-mesh molecular sieve for charcoal production.

2.1.2. Adsorbate BR2

Basic red 2 (BR2), color index 50240, was provided from Carlo Erba, and it was used as taken in the adsorption experiments. BR2 is a positively charged cationic dye and it has a molecular mass of 350.85 g/mol. The synonym name of this dye is safranin-O³⁵ or safranin T.³⁶ Its UPAC name is 3,7-diamino-2,8-dimethyl-5-phenylphenazinium chloride.³⁶ The spectral analysis of BR2 was recorded on a UV-Vis spectrophotometer, and

its absorption spectra recorded for various concentrations are presented (Figure 1). As seen from this figure, the maximum absorbance wavelength of BR2 is 517-520 nm. The molecular structure of BR2 is presented in Figure 2. Some physical properties of BR2 are given elsewhere.^{27,33}

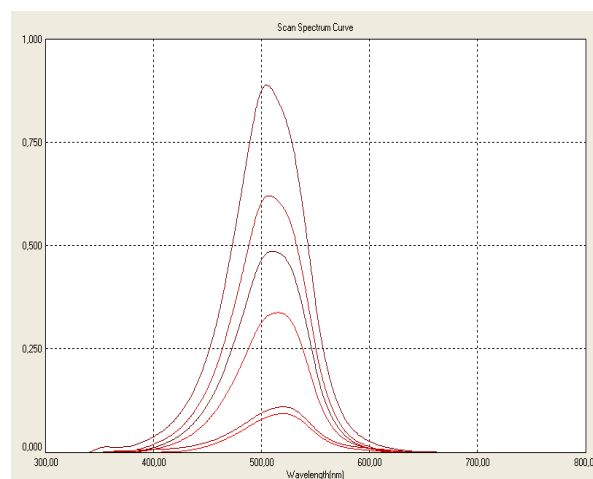


Figure 1. UV-Vis spectra of BR2 (top to bottom concentrations: 150 mg l⁻¹, 100 mg l⁻¹, 75 mg l⁻¹, 50 mg l⁻¹, 20 mg l⁻¹, and 10 mg l⁻¹).

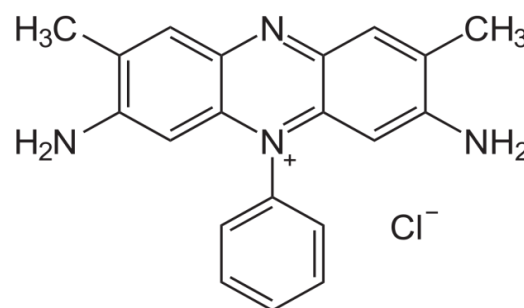


Figure 2. The molecular structure of BR2.

2.1.2.1 Preparation of BR2 solutions

500 mg l⁻¹ stock solution of BR2 was prepared using distilled water. The desired concentrations of BR2 were prepared from the stock. Solution pHs were adapted with diluted HCl and NaOH solutions by a pH meter.

2.2. Methods

2.2.1. Production of the activated biomass charcoal

In this section, firstly charcoal was produced and then the charcoal was activated chemically. The biomass charcoal was produced from peanut shell wastes using pyrolysis system.

This system designed for coal production was manufactured in the industry and shown schematically in Figure 3. The biomass charcoal are produced as stated in our another study.³⁴ Then biomass charcoal obtained was activated chemically as described in the following.

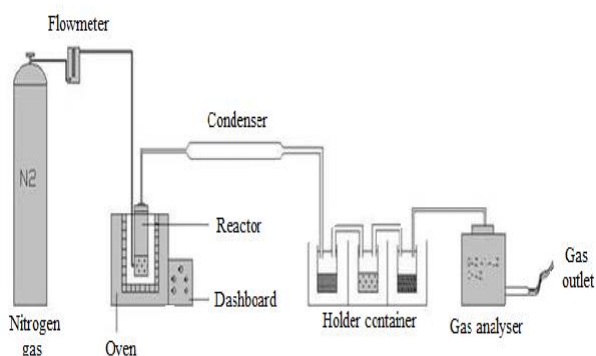


Figure 3. Schematic representation of the pyrolysis system designed for charcoal production.

2.2.1.1. Activation of the biomass charcoal

The biomass charcoal obtained was activated chemically because it did not well adsorb BR2 dye. For this purpose, the biomass charcoal was activated using 1 N NaOH solution as described elsewhere.³⁴ The obtained activated biomass charcoal stored for adsorption experiments.

2.2.3. Characterization of the activated biomass charcoal

Characterization of the activated biomass charcoal was conducted by scanning electron microscopy (SEM), Fourier Transformed Infrared (FT-IR), elemental analyzer, and specific surface area and porosity analyzer. The composition content of the biomass charcoal was performed by an elemental analyzer (LECO CHNS-932 analyzer). Functional groups of the biomass charcoal were determined using a FT-IR spectrophotometer (FTIR RX-1 Perkin Elmer ATR spectrophotometer). Surface morphology of the charcoal was recorded by a SEM (LEO 435 VP SEM). Specific surface area and porosity were measured by a N₂ gas adsorption device (Micromeritics Instrument Corporation).

2.3. Adsorption Experiments

The experiments were conducted by adding 0.25 g of the activated biomass charcoal to 50 ml of BR2 solution in 250-ml erlenmeyers in a temperature-controlled

shaking water bath for different initial BR2 concentrations, temperatures and pHs and at various shaking times at 130 rpm. Following the estimated shaking times, the samples were taken from shaking water bath and centrifuged. After centrifugation, the supernatants were analyzed at 517 nm (maximum wavelength) on T80UV-Vis spectrophotometer.

The percent adsorption (PA) of BR2 from aqueous solution was determined using Eq. (1).

$$PA = \frac{(C_0 - C_t)}{C_0} \times 100 \quad (1)$$

The amount of BR2 removed by the activated biomass charcoal was estimated from Eq. (2).

$$q_t = \frac{(C_0 - C_t) V}{m} \quad (2)$$

where, q_t refers the adsorbed BR2 amount per unit adsorbent mass at any time (in mg g⁻¹). C_0 and C_t show the initial dye concentration and the adsorbed BR2 concentration on the adsorbent at any time (in mg l⁻¹), respectively. V shows the working volume of BR2 solution (in liter), and m indicates mass of the activated biomass charcoal (in gram). At the equilibrium time, $C_t = C_e$ and $q_t = q_e$. C_e is the unadsorbed BR2 concentration in solution at equilibrium time (in mg l⁻¹). q_e indicates the adsorbed BR2 amount per unit of adsorbent mass at the equilibrium time (mg dye per g adsorbent).

2.4. Experimental parameters on the adsorption

2.4.1. Shaking time effect

Shaking times on the adsorption of BR2 by the activated biomass charcoal were selected as 1, 2, 3, 4, 5, 10, 20, 30, 45, 60, 75, 100 min under all experimental parameters in terms of initial dye concentrations, pHs and the temperatures.

2.4.2. Initial dye concentration effect

The initial concentrations on BR2 adsorption by the activated biomass charcoal were selected as 10, 20, 50, 75, 100 and 150 mg l⁻¹ at, 40°C, pH 3 and 130 rpm.

2.4.3. pH effect

The values of solution pH on BR2 adsorption by the activated biomass charcoal were adapted between 3 and 9 for 150 mg l⁻¹ initial concentration at 40°C and 130 rpm. pHs of BR2 solutions were adjusted with dilute sodium hydroxide and hydrochloric acid solutions by a pH meter.

2.4.4. Temperature effect

The temperatures on BR2 adsorption by the activated biomass charcoal were worked between 20 and 60°C for 150 mg l⁻¹ initial concentrations at pH 3 and 130 rpm.

2.5. Column adsorption

Column adsorption works was carried out for the initial concentrations between 10 and 150 mg l⁻¹ at pH 3 and 23°C (at room temperature). The flow rate of BR2 solution was 21 ml h⁻¹.

3. RESULTS AND DISCUSSION

3.1. Characterization of the activated biomass charcoal

3.1.1. Elemental analysis, specific surface area and porosity

As given in our another study,³⁴ the elemental analysis results of the activated biomass charcoal indicate that the activated carbon include 50.34% C, 4.280% H, 2.911% N, and 0.524% S. Specific BET surface area was as found 1.599 m² g⁻¹, and porosity was 0.00195 cm³ g⁻¹.

3.1.2. SEM analysis

The SEM photographs before and after the adsorption are illustrated in Figure 4. As seen from Figure 4a, the surface of the activated carbon is rough, indented and protruding, namely the surface is heterogeneous. After the adsorption of the dye, any change in the heterogeneous structure of the activated biomass charcoal does not occur. Only the surface has become with more blurred image due to dye adsorption (see Figure 4b).

3.1.3. FTIR analysis

FT-IR spectra of the biomass charcoal, the activated biomass charcoal and dye-adsorbed activated biomass charcoal are shown in Figure 5.

The broad band at 3294.84 cm⁻¹ refers -OH groups of glucose and -NH groups of proteins.³⁸ The strong absorption band at 2926.42 indicates aliphatic C-H vibrations.³⁹ After the biomass charcoal was activated with NaOH, the broad band at 3294.84 cm⁻¹ significantly shifted to 3222.09 cm⁻¹ and its intensity remarkably rose. After activation, the peak intensity at 2926.42 cm⁻¹ declined. The peaks at 1434.98 and 1373.71 cm⁻¹ indicate the C = O stretching of carboxylic groups.⁴⁰ After the activation, the peak at 1434.98 diminished. The peak at 1373.71 cm⁻¹ very slightly shifted to 1373.61 cm⁻¹, but this peak broaden and its intensity remarkably ascended. The band at 1574.65 cm⁻¹ probably indicates aromatic C - C stretching.³⁴ After the activation and dye adsorption this peak did not change. After the adsorption

two strong new peaks at 2117.20 and 1216.97 cm⁻¹ occurred. The band at 2117.20 cm⁻¹ probably indicates C = C stretching due to the structure of the dye after the adsorption. Band at 1216.97 cm⁻¹ probably shows C-H stretching in the structure of the dye.³⁴ After the activation, a new band at 1065.16 cm⁻¹ appeared. This band probably refers to the out of-plane bending for carbonates in the activated biomass charcoal.⁴¹ After BR2 adsorption, this band greatly shifted to 1013 cm⁻¹. The peaks at < 1000 cm⁻¹ indicate fingerprint zone resulted from sulfur or phosphate,²⁷ and these peaks did not almost change after the carbonization and the dye adsorption. FT-IR results imply that a chemical interaction may have taken place between the functional groups on the surface of the activated biomass charcoal and positively charged BR2 molecules.

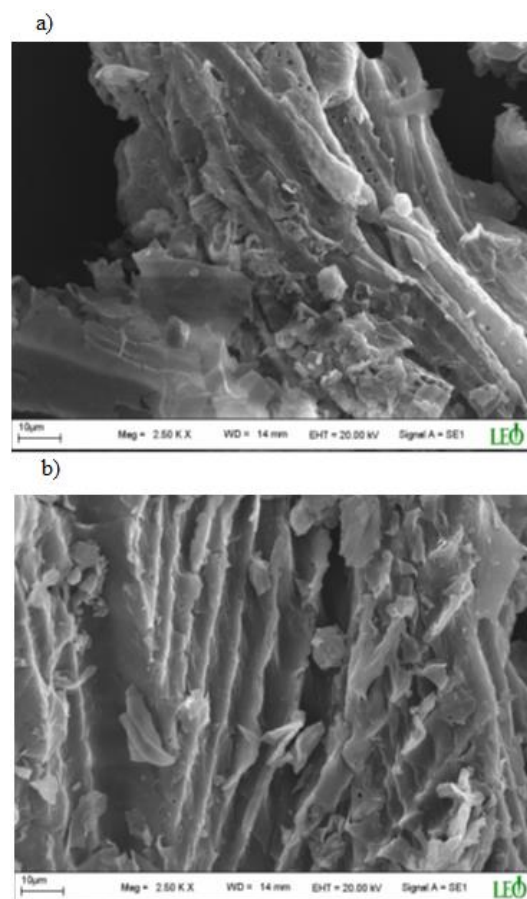


Figure 4. The SEM images, a) the activated biomass charcoal before adsorption, b) dye-adsorbed activated biomass charcoal after adsorption.

3.2. Shaking time effect and the adsorption equilibrium time

Effect of shaking time on BR2 adsorption was studied for different initial BR2 concentration, pH and temperature at different shaking times. The maximum adsorption was attained at 5 min under all the experimen-

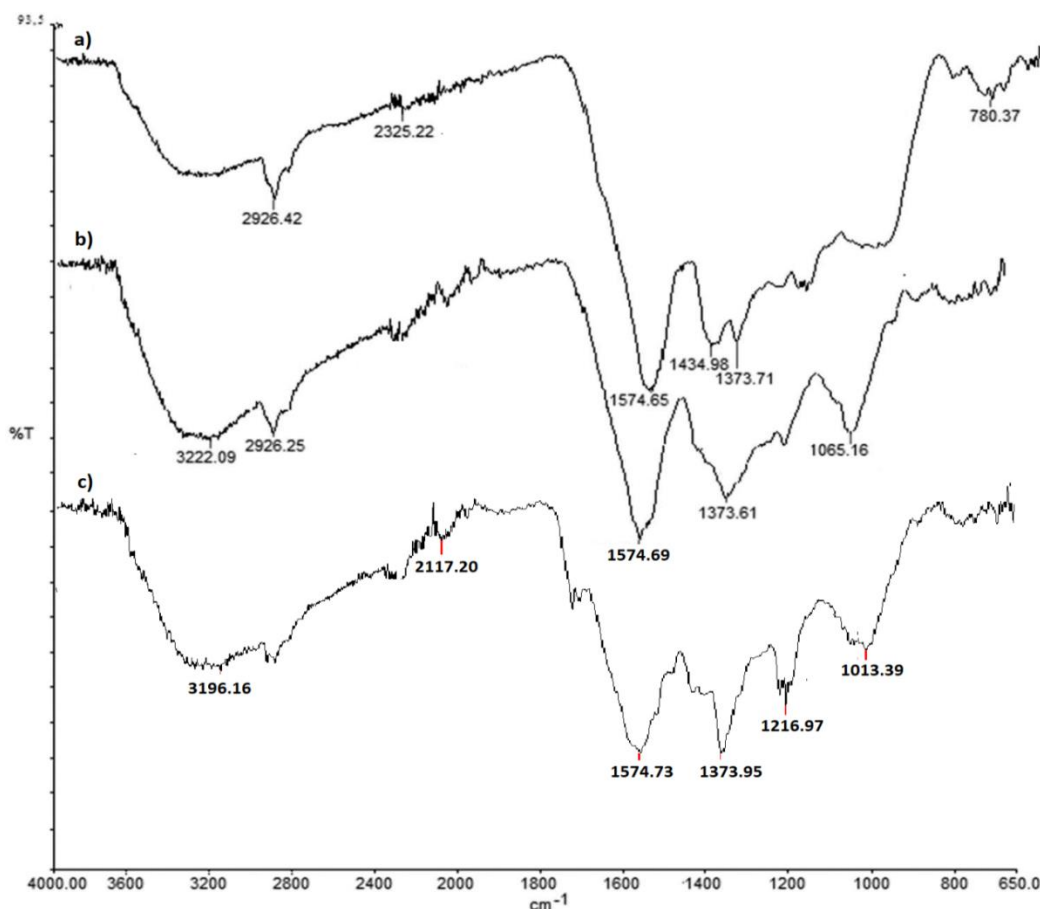


Figure 5. FT-IR spectra: a) the biomass charcoal, b) the activated biomass charcoal, c) dye-adsorbed activated biomass charcoal.

tal conditions. After 5 min, any increase in the adsorption did not observe. Therefore, the equilibrium time of the adsorption was determined as 5 min.

3.3. Initial dye concentration effect

Figure 6 demonstrates the effect of initial dye concentration on the adsorption. As seen from the figure, it was determined that BR2 was highly adsorbed by the activated biomass charcoal from the first minutes and reached the maximum level at 5 min. There was no change in the adsorption after 5 min. The maximum adsorption (ie. adsorbent capacity) at 5 min was found as 1.958 mg g⁻¹ (97.93%), 3.903 mg g⁻¹ (97.59%), 9.913 mg g⁻¹ (99.13%), 14.826 mg g⁻¹ (98.84%), 19.853 mg g⁻¹ (99.26%), and 29.868 mg g⁻¹ (99.56%) for all concentrations between 10 and 150 mg l⁻¹, respectively. This refers a very rapid interaction between the activated biomass charcoal and BR2 molecules. In addition, it was observed that the red color of BR2 completely disappeared and became clear from the first minute. This situation was also observed in pH and temperature

studies. A similar situation has been observed for BR2 adsorption onto peanut shell.²⁷

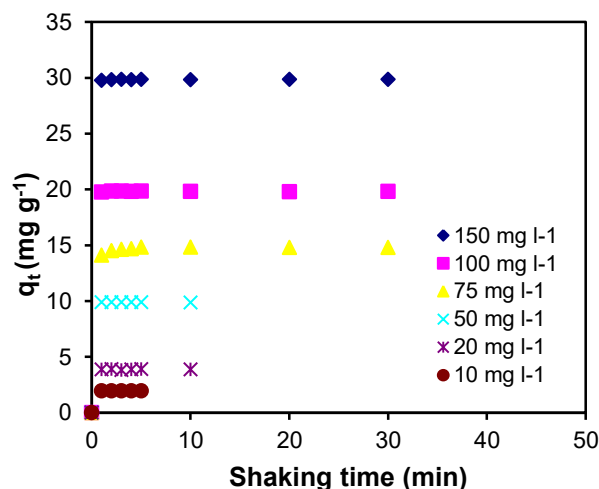


Figure 6. The effect of initial BR2 concentration on the adsorption (pH: 3, T: 40°C, w/v: 0.25g/50 ml).

3.4. pH effect

Figure 7 illustrates pH effect on BR2 adsorption by the activated biomass charcoal.

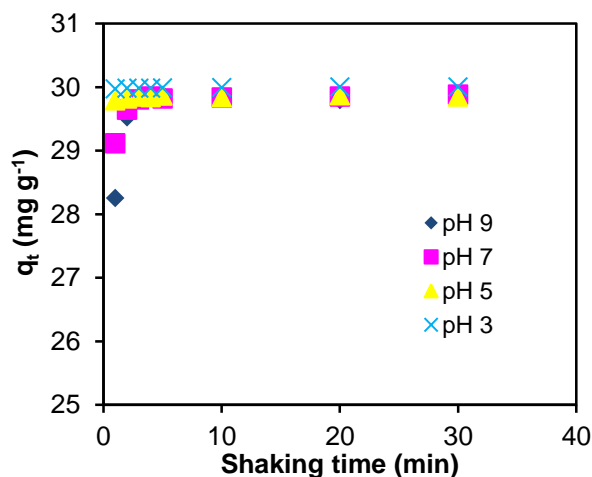


Figure 7. pH effect on BR2 adsorption (C_0 : 150 mg l⁻¹, T: 40°C, w/v: 0.25g/50 ml).

As seen from Figure 7, a very high adsorption was observed at all pH values from the first minutes and it was observed that it reached the maximum level at 5 min. The maximum adsorption (i.e. the adsorbent capacity) at pH 3, 5, 7 and 9 within 5 min was determined as 29.983 mg g⁻¹ (99.91%), 29.864 mg g⁻¹ (99.54%), 29.817 mg g⁻¹ (99.39%) and 29.874 mg g⁻¹ (99.58%), respectively. It was considered that it was suitable to study at any pH value, since the adsorbed amounts at each pH were very high and very close to each other. As seen from this figure, it was observed that pH had no effect on the maximum adsorption.

3.5. Temperature effect

Figure 8 demonstrates temperature effect on BR2 adsorption by the activated biomass charcoal. From this figure, it is seen that the maximum adsorption slightly rise with increasing the temperature. The most adsorption was observed to occur at 60°C. While the adsorption in the first min at 20 and 30°C was 12.42 mg g⁻¹ (82.84%) and 13.17 mg g⁻¹ (87.86%), the maximum adsorption (i.e. the adsorbent capacity) was found as 14.89 mg g⁻¹ (99.65%) and 14.89 mg g⁻¹ (99.28%) in 5 min, respectively. On the other hand, the adsorption within the first 5 min at 40, 50 and 60°C was very close to each other and the maximum adsorption was reached within 5 min. The maximum adsorption (i.e. the adsorbent capacity) at 40 and 60°C was estimated as 29.86 mg g⁻¹ (99.56%) and 29.94 mg g⁻¹ (99.80%), respectively. The maximum adsorption at 40°C

and 60°C are very close to each other, and the maximum adsorption are determined as 14.84 mg g⁻¹ (98.84%) and 14.94 mg g⁻¹ (99.60%), respectively.

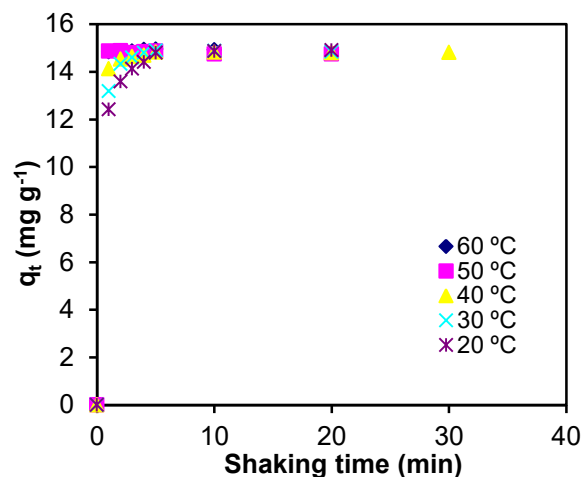


Figure 8. Temperature effect on BR2 adsorption (C_0 : 150 mg l⁻¹, pH: 3, w/v: 0.25g/50 ml).

3.6. Column adsorption study

The operating conditions for the column adsorption are summarized in Table 1. The system was operated at 23°C and pH 3. As can be seen from this table, a glass column with 1 cm diameter and 20 cm length was used for the continuous adsorption system. 2 g dry weight of activated biomass charcoal particles were packed between two layers of glass wool in the column. BR2 solution with the predetermined concentrations was fed through the top of the column. The flow rate of feed solutions was regulated as 0.35 ml min⁻¹ (21 ml h⁻¹). The dye samples passed through the column were collected from the bottom of the column at specific times. The samples from the outlet of the column were analyzed by UV-Vis spectrophotometer. The values of percent adsorption of BR2 by the column are shown in Figure 9.

Table 1. Column operating conditions

| | |
|-----------------------------------|--------|
| Column diameter, cm | 1 |
| Column length, cm | 20 |
| Height of bed, cm | 10 |
| Packing size, mesh | 100 |
| Flow rate, ml h ⁻¹ | 21 |
| Concentration, mg l ⁻¹ | 10-150 |
| Temperature, °C | 23 |
| Solution pH | 3 |

Table 2. Kinetic parameters

| | | Intra-particle diffusion | | | Pseudo-first order kinetics | | | Pseudo-second order kinetics | | |
|-----------------------|-----------------------|---|--------|--------|-----------------------------|----------------------|-------|------------------------------|---|-------|
| C_o | q_e (exp) | k_i | r^2 | C | q_1 | k_1 | r^2 | q_2 | k_2 | r^2 |
| (mg l ⁻¹) | (mg g ⁻¹) | (mg g ⁻¹ min ^{-1/2}) | | | (mg g ⁻¹) | (min ⁻¹) | | (mg g ⁻¹) | (mg g ⁻¹ min ⁻¹) | |
| 10 | 1.95 | 0.0018 | 0.0354 | 1.9575 | 0.003 | 0.03 | 0.002 | 1.95 | 523.05 | 1 |
| 20 | 3.90 | 0.0091 | 0.0137 | 3.8861 | 0.017 | 0.03 | 0.001 | 3.87 | 111.02 | 0.999 |
| 50 | 9.91 | 0.0043 | 0.0472 | 9.9113 | 0.004 | 0.05 | 0.004 | 9.91 | 11.31 | 1 |
| 75 | 14.82 | 0.5571 | 0.8905 | 13.638 | 1.015 | 0.52 | 0.943 | 14.88 | 1.32 | 1 |
| 100 | 19.85 | 0.0651 | 0.5632 | 19.719 | 0.063 | 0.39 | 0.291 | 19.84 | 25.40 | 1 |
| 150 | 29.86 | 0.0582 | 0.8063 | 29.734 | 0.101 | 0.43 | 0.598 | 14.02 | 14.02 | 1 |

As seen from Figure 9, the column adsorption of BR2 was determined to be between 99.17 and 99.47% for all the concentrations. Besides it was observed that all the outlet samples are colourless and cleared off the red colour of BR2. This situation indicates a high affinity between the functional groups of BR2 molecules and activated biomass charcoal packed in column. Column exhaustion time was determined as 15.5 h. When the flow rate is doubled (ie. 0.70 ml min⁻¹ (42 ml h⁻¹)), the adsorption was found to be 99.50%. At the same time, when the flow rate is worked as 0.70 ml min⁻¹, the accumulation of dye solution in the column was observed. Therefore, it was seen that an increase in the flow rate had no effect on the column adsorption. Based on this, the flow rate was not further increased.

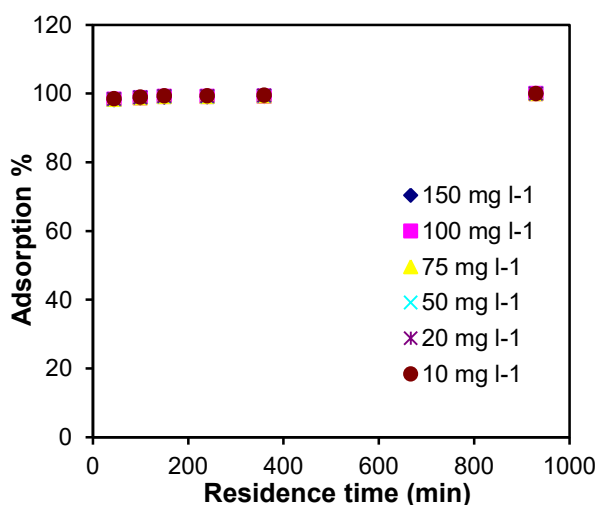


Figure 9. Initial BR2 concentration effect on the column adsorption. (C_o : 150 mg l⁻¹, pH: 3, w: 2 g, v: 50 ml, flow rate: 21 ml h⁻¹).

3.7. Kinetic study

Adsorption kinetics was examined according to three commonly used models. The intra-particle diffusion model suggested by Weber and Morris is given in Eq. (3).⁴²

$$q_t = k_i t^{1/2} + C \quad (3)$$

The pseudo-first order kinetic model proposed by Lagergren is presented in Eq. (4).⁴³

$$\log (q_e - q_t) = \log q_1 - \frac{k_1}{2.303} t \quad (4)$$

The pseudo-second order kinetic model put forward by Ho and McKay is given in Eq. (5).⁴⁴

$$\frac{t}{q_t} = \frac{1}{k_2 q_2^2} + \frac{1}{q_e} t \quad (5)$$

where, k_i implies the intra-particle diffusion rate constant. k_1 and k_2 indicate the rate constants for the pseudo-first and -second order models, respectively. q_t and q_e indicate the amounts adsorbed of BR2 per unit of the adsorbent at any time and equilibrium time, respectively. The term $k_2 q_2^2$ indicates initial adsorption rate and is represented with h . All kinetic studies were conducted for the initial BR2 concentrations between 10 and 150 mg l⁻¹ at pH 3 and 40°C. The obtained all kinetic parameters are submitted in Table 2.

Firstly, the plots of q_t against $t^{1/2}$ for the intra-

particle diffusion were obtained. The values of coefficient of determination (r^2) from the linear regression analysis of the plots obtained were determined as 0.0354, 0.0137, 0.0472, 0.8975, 0.5632, and 0.8063 for the initial concentrations of 10, 20, 50, 75, 100, and 150 mg l⁻¹, respectively. These low values show that the adsorption does not follow the intra-particle diffusion model. Due to the low r^2 values, the plots are not given here. However, due to the surface adsorption, the boundary layer thickness (the value C) was determined to be rose with increasing initial dye concentration (see Table 2).

Secondly, the plots of $\log(q_e - q_t)$ against t for the pseudo-first order model were drawn. The values of the r^2 from the linear regression analysis of the plots were found as 0.0026, 0.0013, 0.0045, -0.9435, 0.2916, and 0.5989 for the initial concentrations of 10, 20, 50, 75, 100, and 150 mg l⁻¹, respectively. As seen, the r^2 values are very low. Also, there is no any harmony between the experimental adsorption capacities (q_{exp}) and theoretical adsorption capacities (q_i) from the pseudo-first order model. Therefore, the adsorption is not consistent with the pseudo-first order kinetic model. Due to low r^2 values, the plots are not given here. Finally, the linear plots of t/q_t against t for the pseudo-second order model were drawn (see Figure 10).

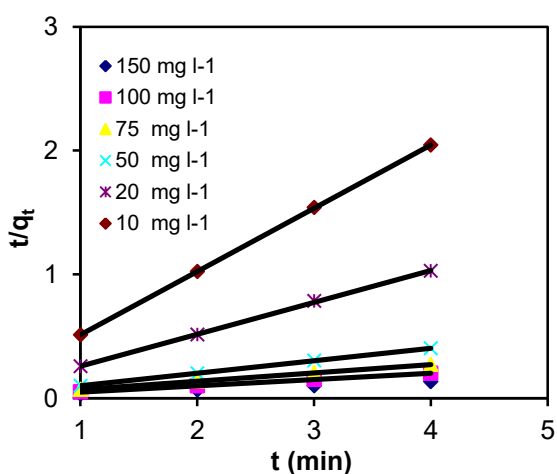


Figure 10. Concentration effect on the pseudo-second order kinetics.

From the regression analyses above, the values of the r^2 are very high. The values of r^2 are 1 for all initial concentrations between 10 and 150 mg l⁻¹ (except for 20 mg l⁻¹). At the same time, there is a harmony between the experimental adsorption capacities (q_{exp}) and theoretical adsorption capacities (q_2) from the pseudo-second order model (see Table 2). Therefore, the adsorption obeyed the pseudo-second order kinetics.

This situation may be inscribed to a chemical activation between BR2 dye molecules and the functional active sites of adsorbent. Similar findings have been noted for safranin adsorption by peanut shell,²⁷ carbonized spent coffee ground,⁴⁵ and kaolinite clay.⁴⁶

3.8. Isotherm study

Adsorption isotherm was investigated by the Langmuir and Freundlich models used commonly given elsewhere.^{3,16} According to isotherm analyses results, it is seen that the plot of C_e/q_e versus C_e is a contrary to the Langmuir model. However, the isotherm is in consistent with the Freundlich model. The k and n values were estimated from the intercept and slope of the plot of $\ln q_e$ against $\ln C_e$, respectively. The values of k and n were determined as 29.34 mg g⁻¹ and 0.58 g l⁻¹, respectively. The r^2 value for the Freundlich isotherm was estimated as 0.74. This low r^2 indicates a partial compatibility to the Freundlich model, which shown a randomness adsorption of the dye molecules on the adsorbent surface. A similar result has been noted for BR2 adsorption by peanut shell.²⁷

4. CONCLUSIONS

In this study, the charcoal was produced from peanut shells and then this charcoal was activated chemically with sodium hydroxide. The activated biomass charcoal obtained was used as an adsorbent in removing BR2, a cationic dye from aqueous solution in batch and column systems. The maximum adsorption of BR2 by the activated biomass charcoal (i.e. adsorbent capacity) was determined to be 99.91% and 99.50% in batch and column systems, respectively. It was seen that the adsorption obeyed the Freundlich isotherm and the pseudo-second order kinetic model. At the same time, a surface adsorption was estimated to be occurred on the heterogeneous adsorbent surface. Alternative to commercial activated carbon, the activated biomass charcoal produced from peanut shell was determined to be used easily for the adsorption of BR2 dye, a cationic dye.

ACKNOWLEDGEMENTS

This study was supported by The Scientific and Technical Research Council of Turkey (TUBITAK), project number: 107Y043.

Conflict of interest

Authors declare that there is no a conflict of interest with any person, institute, and company, etc.

REFERENCES

1. Argun, M. E.; Dursun, S.; Gur, K.; Ozdemir, C.; Karatas, M.; Dogan, S. *Environ Technol.* **2005**, 26, 479-487.
2. Acemioğlu, B.; Alma, M. H. *Fresenius Environ. Bull.* **2004**, 13(7), 585-590.
3. Acemioğlu, B.; Alma, M. H.; Demirkıran, A. R. *J. Chem. Soc. Pak.* **2004**, 26 (1), 82-89.
4. Acemioğlu, B. *Bioresour. Technol.* **2004**, 93, 99-102.
5. Hamdaoui, O.; Saoudi, F.; Chida, M.; Naffrechoux, E. *Chem. Eng. J.* **2008**, 143, 73-84.
6. Yagub, M. T.; Sen, T. K.; Ang, H. M. *Water Air Soil Pollut.* **2012**, 223, 5267-5282.
7. Deniz, F.; Karaman, S. *Chem. Eng. J.* **2011**, 170, 67-74.
8. Ofomaja, A. E.; Ho, Y. S. *Bioresour. Technol.* **2008**, 99, 5411-5417.
9. Mane, V. S.; Vijay Babu, P. V. *Desalination* **2011**, 273, 321-329.
10. Witek-Krowiak, A. *Chem. Eng. J.* **2011**, 171, 976-985.
11. Dulman, V.; Cucu-Man, S. M. *J. Hazard. Mater.* **2009**, 162, 1457-1464.
12. Acemioğlu, B.; Alma, M. H. *Holz Roh Werkst.* **2004**, 62, 268-272.
13. Ning-Chuan, F.; Xue-yi, G. *Trans. Nonferrous Met. China*, **2012**, 22, 1224-1231.
14. Annadurai, G.; Juang, R. S.; Lee, D. J. *J. Hazard. Mater.* **2002**, B92, 263-274.
15. Sartepe, A. S.; Mandhare, A. M.; Jadhav, V. V.; Raut, P. D.; Anuse, M. A.; Kolekar, S. S. *Arabian J. Chem.* **2017**, 10, 3229-3238.
16. Kule, L.; Acemioğlu, B.; Baran, E. *Int. J. Chem. Technol.* **2017**, 1, 58-66.
17. Pagnenelli, F.; Mainelli, S.; Veglio, F.; Toro, L. *Chem. Eng. J.* **2003**, 4709-4717.
18. Hodaifa, G.; Driss Alami, S. B.; Ochando-Pulido, J. M.; Victor-Ortega, M. D. *Ecol. Eng.* **2014**, 73, 270-275.
19. Dagdelen, S.; Acemioğlu, B.; Baran, E.; Koçer, O. *Water Air Soil Pollut.* **2014**, 225 (3) Article Number: 1899, 1-15.
20. Koçer, O.; Acemioğlu, B. *Desalin. Water Treat.* **2016**, 57 (35) 16653-16669.
21. Öncel, M.; Guvenç, İ.; Acemioğlu, B. *Asian J. Chem.* **2012**, 24 (4), 1698-1704.
22. Duran, C.; Ozdes, D.; Gundogdu, A.; Senturk, H. B. *J. Chem. Eng. Data.* **2011**, 56 (5), 2136-2147.
23. Doğan, M.; Abak, H.; Alkan, M. *J. Hazard. Mater.* **2009**, 164, 172-181.
24. Ding, D.; Zhao, Y.; Yang, S.; Shi, W.; Zhang, Z.; Lei, Z.; Yang, Y. *Water Res.* **2013**, 47, 2563-2571.
25. Robinson, T.; Chandaran, B.; Nigam, P. *Bioresour. Technol.* **2002**, 85, 119-124.
26. Wafwoyo, W.; Seo, C. W.; Marshall, W. E. *J. Chem. Technol. Biotechnol.* **1999**, 74, 1117-1121.
27. Şakalar, N.; Bilir, M. H.; Acemioğlu, B.; Alma, M. H. *Asian J. Chem.* **2010**, 22 (7) 5649-5662.
28. Şamil, A.; Acemioğlu, B.; Gültekin, G.; Alma, M. H. *Asian J. Chem.* **2011**, 23 (7), 3224-3230.
29. Akkoc, Y.; Acemioğlu, B. *Fresenius Environ. Bull.* **2018**, 27 (12A), 9357-9365.
30. Karaoğlu, M. H.; Uğurlu, M. *Fresenius Environ. Bull.* **2010**, 19 (12b), 3199-3208.
31. Acemioğlu, B.; Şakalar, N. *Fresenius Environ. Bull.* **2017**, 26 (8), 5305-5313.
32. Bilir, M. H.; Şakalar, N.; Acemioğlu, B.; Baran, E.; Alma, M. H. *J. Appl. Polym. Sci.* **2013**, 4340-4351.
33. Acemioğlu, B.; Bilir, M. H.; Alma, M. H. *Int. J. Chem. Technol.* **2018**, 95-104.
34. Acemioğlu, B. *Int. J. Coal Prep. Util.* **2019**, <https://doi.org/10.1080/19392699.2019.1644326>
35. Kumar, K. V. *J. Hazard. Mater.* **2007**, 142, 564-567.
36. Zaghbani, N.; Hafiane, A.; Dhahbi, M. *Desalination* **2008**, **222**, 348-356.
37. Wakkal, M.; Khiari, B.; Zagrouba, F. *Environ. Sci. Pollut. Res.* **2019**, 26, 18942-18960.

DOI: <http://dx.doi.org/10.32571/ijct.650476>

E-ISSN:2602-277X

38. Dmitrienko, S. G.; Siviridova, O. A.; Pyatkova, L. N.; Senyamin, V. M. *Anal. Bioanal. Chem.* **2002**, 374(3), 361-368.

39. Hameed, B. H.; Mahmoud, D. K.; Ahmad, A.L. *J. Hazard. Mater.* **2008**, 158(2-3) 499-506.

40. Bayramoğlu, G.; Arica, M. Y. *J. Hazard. Mater.* **2007**, 143(1-2), 135-143.

41. Xu, R. K., S. C. Xiao, J. H. Yuan, and A. Z. Zhao. *Bioresour. Technol.* **2011**, 102, 10293-10298.

42. Weber, W. J. Morris, J.C. *J. Sanit Eng. Div.* 1963, **89** (SA2), 31-59.

43. Lagergren, S. K. *Sven. Vetenskapsakad. Handl.* Band 24, 1-39.

44. Ho, Y.S.; McKay, G. *Chem. Eng. J.* **1998**, 70, 115-124.

45. Lakshmi Prasanna, M.; Sumithra, S.; Madakka, M. *Int. J. Recent Sci. Res.* **2016**, 7(4), 10401-10405.

46. Adebawale, K. O.; Olu-Owalabi, B. I.; Chigbundu. C. E. *J. Encapsulation Adsorpt. Sci.* **2014**, 4, 89-104.

ORCID

 <https://orcid.org/0000-0002-0728-2747> (B. Acemioğlu)

 <https://orcid.org/0000-0001-7415-1088> (N. Karataş)

 <https://orcid.org/0000-0001-9987-1882> (M. H. Güler)

 <https://orcid.org/0000-0001-9218-5513> (M. Ertaş)

 <https://orcid.org/0000-0001-6323-7230> (M. H. Alma)